Food Chemistry: X 23 (2024) 101605

Contents lists available at ScienceDirect

Food Chemistry: X

journal homepage: www.sciencedirect.com/journal/food-chemistry-x

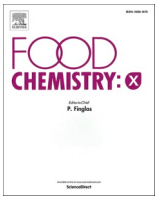

Establishment of an amplification strategy - specific binding - convenient processing integrated aflatoxin B1 detection method based on Fe_3O_4-NH_4/AuNPs/apt-S1

Hua Zheng [a,1], Linlin Feng [b,g,1], Zheng Huang [c], Ziwei Zou [b], Xiaolong Ma [a], Ziping Pan [b], Jinfeng Li [b], Jinxia Wu [b,**], Mei Li [b,**], Zhiheng Su [b,d,e,f,*]

[a] Institute of Life Sciences, Guangxi Medical University, Nanning 530021, China
[b] Pharmaceutical College, Guangxi Medical University, Nanning 530021, China
[c] Guangxi Nanning First People's Hospital, Nanning 530016, China
[d] Guangxi Key Laboratory of Bioactive Molecules Research and Evaluation, Guangxi Medical University, Nanning 530021, China
[e] Guangxi Beibu Gulf Marine Biomedicine Precision Development and High-value Utilization Engineering Research Center, Guangxi Medical University, Nanning 530021, China
[f] Guangxi Health Commission Key Laboratory of Basic Research on Antigeriatric Drugs, Guangxi Medical University, Nanning 530021, China
[g] Liuzhou People's Hospital afliated to Guangxi Medical University, Liuzhou 545006, Guangxi, China

ARTICLE INFO

Keywords:
Aflatoxin B1
Electrochemistry
Amplification strategy
Peanut oil

ABSTRACT

Aflatoxin B1 (AFB1) is a potent toxin in food, necessitating rapid, instant, and sensitive detection. We have engineered an electrochemical sensor to monitor AFB1 using a system composed of Fe_3O_4-NH_4/AuNPs/apt-S1. The aptamer specifically recognizes AFB1, while 'S1' is functionalized with methylene blue to enhance the current. The RecJf exonuclease promotes the formation of the electrochemical strategy. The Fe_3O_4 component, with its magnet properties, enables a rapid separation of solids and liquids without the need for instrumentation. The sensor exhibits a linear range for AFB1 ranging from 1 ng to 10 μg. The regression equation is I(nA) = 446.8 × logc+2085 (where I and c represent the peak current and AFB1 concentration, respectively). The correlation coefficient is 0.9508, and the detection limit is 3.447 nM. The relative standard deviation of AFB1 in peanut oil ranges from 4.80% to 6.80%. These results demonstrate that the sensor has high sensitivity, stability, repeatability, and specificity for AFB1 detection.

1. Introduction

About 20 derivatives of the aflatoxin family, including B1, B2, G1, and G2, with the most common types ranked by toxicity as AFB1 > AFM1 > AFG1 > AFB2 > AFG2 (Abdolmaleki et al., 2022). The International Agency for Research on Cancer (IARC) classifies AFB1 as a Group 1 and 2B human carcinogen due to its hepatocarcinogenic, mutagenic, and genotoxic properties (Lei, Zhang, & Qi, 2013; Marchese et al., 2018). AFB1 is commonly found in numerous food products, such as milk, seed-based foods, and fatty oils. Excessive ingestion of aflatoxin can damage tissues and organs, potentially leading to cancer, teratogenesis, mutations, and even death (Chavarría et al., 2017; Rushing & Selim, 2019).

Peanut oil, the fifth most extensively used oil in confectionery factories, candies, and pastries, is rich in fatty acids and carbohydrates, offering high nutritional and commercial value (Tosun & Ayyıldız, 2013). However, peanut oil is also prone to aflatoxin contamination. The study indicated that the pooled prevalence of AFB1 in peanut oil is 47.9%; AFB2, 46.45%; AFG1, 46.92%, and AFG2, 54.01% (Fakhri, Omar, Mehri, Hoseinvandtabar, & Mahmudiono, 2023). China is the world's largest market for the production and consumption of peanuts and their derivatives, particularly peanut oil (Dean, 2021). The National Standard of the People's Republic of China (GB 2761–2017) sets a limit of 20 μg/kg for AFB1 in peanut oil. Permissible limits for AFB1 in food range from 0 to 40 parts per billion (ppb), while the level in animal feeds is about 300 ppb (Fasihi-Ramandi, Bayat, Kachuei, & Golmohammadi,

* Corresponding author at: Pharmaceutical College, Guangxi Medical University, Nanning 530021, China.
** Corresponding author.
E-mail addresses: jinxia-wu@sr.gxmu.edu.cn (J. Wu), gxlimei@126.com (M. Li), suzhiheng915@126.com (Z. Su).
[1] These authors share first authorship.

https://doi.org/10.1016/j.fochx.2024.101605
Received 9 May 2024; Received in revised form 27 June 2024; Accepted 28 June 2024
Available online 1 July 2024

2023). Wild et al. stated that human ingestion of AFB1 at doses of approximately 20–100 μg·kg^{-1} bw per day for 1–3 weeks could result in toxicity or death (Wild and Gong, 2010). Consequently, rapid detection of AFB1 in peanut oil is imperative to safeguard public health and maintain stringent food quality control.

Conventional methods for detecting AFB1 in food mainly involve techniques such as High-Performance Liquid Chromatography (HPLC), Isotope Dilution Liquid Chromatography Tandem Mass Spectrometry (ID-LC-MS/MS), Enzyme-Linked Immunosorbent Assay (ELISA), and Thin Layer Chromatography (TLC). However, these methods have disadvantages such as laborious sample preparation, high cost, complex data analysis, and the need for professional testing. Therefore, developing a convenient, rapid, and economical method to detect AFB1 is important.

Electrochemical biosensors offer good selectivity, high sensitivity, and simple operation, making them one of the most commonly employed detection methods in scientific research (Xu, Wang, Ding, & Luo, 2021). Aptamers (apt) are single-stranded DNA or RNA oligonucleotide sequences characterized by high affinity and specificity for the target, low cost, easy modification, and high stability (Qian et al., 2018; Wang et al., 2018). Gold nanoparticles (AuNPs) have unique optoelectronic, physical, and chemical properties, along with biocompatibility and easy functionalization with various ligands (Wang, Ding, Zhang, & Jiang, 2023). The terminal ends of aptamers are usually modified with disulfide groups, amino groups, ferrocene, and thiols, which can be readily bound to electrode surfaces or gold nanoscale (Wu, Baker, & Lai, 2017; Wu & Lai, 2017). Self-assembly of thiol-terminated oligonucleotides on gold surfaces can be achieved mainly through the formation of Au-S bond covalent linkages, a direct and simple method of oligonucleotide functionalization of gold nanosurfaces (Tani, Thomson, & Butt, 2001).

Methylene blue (MB) is a phenothiazine that can interact with DNA in three modes: intercalation, groove binding, and electrostatic binding (Khadieva et al., 2021; Vardevanyan, Antonyan, Parsadanyan, Shahinyan, & Petrosyan, 2021; Zhang & Tang, 2004). Due to its good solubility and strong redox signal, MB is widely used for labeling DNA sequences or as an electrochemical signal generator for insertion into DNA single or double strands (Abedi, Raoof, Mohseni, & Bagheri Hashkavayi, 2023; Han, Liu, Yang, & Wang, 2019; Miao et al., 2016). The interaction between the target and the aptamer causes changes in the distance between the electrochemical label and the electrode surface, affecting electron transfer efficiency (Yu, Sutlief, & Lai, 2018).

Therefore, we aim to fabrication of an electrochemical sensor that enables the rapid separation and detection of AFB1 in peanut oil. First, an electrochemical signal amplification system will be established for the cyclic reaction of Fe_3O_4-NH_4/AuNPs/apt-S1 and AFB1. The aptamer specifically recognizes AFB1, while 'S1' is functionalized with MB to enhance the electrical signal. RecJf exonuclease facilitates electrochemical signal amplification. The incorporation of Fe_3O_4-NH_4 nanoparticles serves a dual purpose: providing a platform for the immobilization of AuNPs and aptamers and enabling quick separation of the solid-liquid mixture due to its magnetic properties. We then aspirate the supernatant solution to detect its electrical signal. This study will provide a promising method for the conventional detection of AFB1 in peanut oil.

2. Materials and methods

2.1. Chemical reagents

Chloroauric acid was purchased from Dulei Biotechnology Co. Ltd. (Nanjing, China). Sodium hydroxide was acquired from the Tianjin Damao Chemical Reagent Factory (Tianjin, China). Trisodium citrate was purchased from Chengdu Kelong Chemical Reagent Factory (Chengdu, China). The aptamer (5′ to 3′, AGTTGGG CACGTGTTGTCTCTCTCTGTGTCTCGTGCCCTTCGCTAGGCCCACA-SH) (Tan et al., 2019) and complementary strand DNA (S1, 5′ to 3′, GACAACACGTGCCCAACT-MB) were obtained from Shanghai Sangong Bioengineering Co. Ltd. (Shanghai, China). Ferric chloride hexahydrate, ferrous chloride tetrahydrate, n-hexane, and trifluoroacetic acid were sourced from Aladdin Biochemistry and Technology Co. Ltd. (Shanghai, China). RecJf exonuclease was acquired from Beyotime Biotechnology Co. Ltd. (Shanghai, China). Aflatoxin B1 was procured from Shanghai McLean Biochemical Science and Technology Co. Ltd. (Shanghai, China). Aflatoxins B2, M1, G1, and G2 were purchased from Shanghai Yuanye Biotechnology Co. Ltd. (Shanghai, China).

2.2. Instruments

This study utilized a portable electrochemistry workstation IGS1200 (China) with iLAB portable electrochemistry software, a UV–Vis photometer (Agilent CARY3500, USA), a multifunctional enzyme labeling instrument (Berten Instruments Ltd., Synergy H1, USA), a High-Performance Liquid Chromatography instrument (HPLC) (Agilent Technologies Ltd. 1260 Infinity II), a transmission electron microscope (Hitachi H7650), a vibrating sample magnetometer (LakeShore7404, USA), and a scanning electron microscope (SEM) (TESCAN, Czech Republic) MIRA LMS).

2.3. Synthesis of Fe_3O_4-NH_4/AuNPs

Synthesis of gold nanoparticles: 1 mL of 1% chloroauric acid was added to 100 mL of ultrapure water and heated to boiling with continuous stirring. Then, 1.5 mL of 1% trisodium citrate was rapidly added, and the mixture was stirred for 15 min. The color of the solution gradually changed from grey to black and then to a stable purplish red (Frns, 1973Frens, 1973).

Synthesis of Fe_3O_4-NH_4 (Fang, Chen, Zhang, & Chen, 2016; Guan et al., 2019; Wang et al., 2014): 1 g of prepared Fe_3O_4NPs was ultrasonically dispersed in 50 mL of a 20% ethanol solution. Then, 1 mL of (3-aminopropyl)-triethoxysilane (APTES) was added. A black suspension with fine particles was obtained by sufficiently oscillating the mixture for 10 h at room temperature in a water oscillating shaker at 150 r/min, producing amino-carbonated magnetic Fe_3O_4NPs. The resulting nanoparticles were separated, washed three times with a 20% ethanol solution, and dried for future use.

2.4. Establishment of standard curve

The electrochemistry test was conducted using a screen-printed electrode setup consisting of a saturated silver-silver chloride (Ag/AgCl) reference electrode, a platinum counter electrode, and a working electrode. The test parameters for the electrochemistry were: scanning region: −0.4 to −1.1 V, scanning rate: 50 mV/s, and resting time: 2 s. Under optimal experimental conditions, differential pulse voltammetry (DPV) was used to determine the reduction peak currents of AFB1 at various concentrations (1 ng/mL, 2 ng/mL, 5 ng/mL, 10 ng/mL, 100 ng/mL, 1000 ng/mL, and 10,000 ng/mL) in a 0.1 M KCl solution. A standard curve was established by studying the relationship between current values and AFB1 concentration.

2.5. Pre-treatment and testing conditions for peanut oil

The treatment and detection methods were mainly based on the determination of aflatoxins B and G in foods according to national food safety standards (GB5009.22–2016), with appropriate adjustments. Sample extraction: 5 g of peanut oil (accurate to 0.01 g) was weighed into a 50 mL centrifuge tube. Then, 20 mL of a methanol-water solution (v: v, 7:3) was added, vortexed, mixed well, and placed on a shaking table for 20 min. The mixture was centrifuged at 6000 r/min for 15 min, and the supernatant was reserved.

The derivatization method described in the study involves the

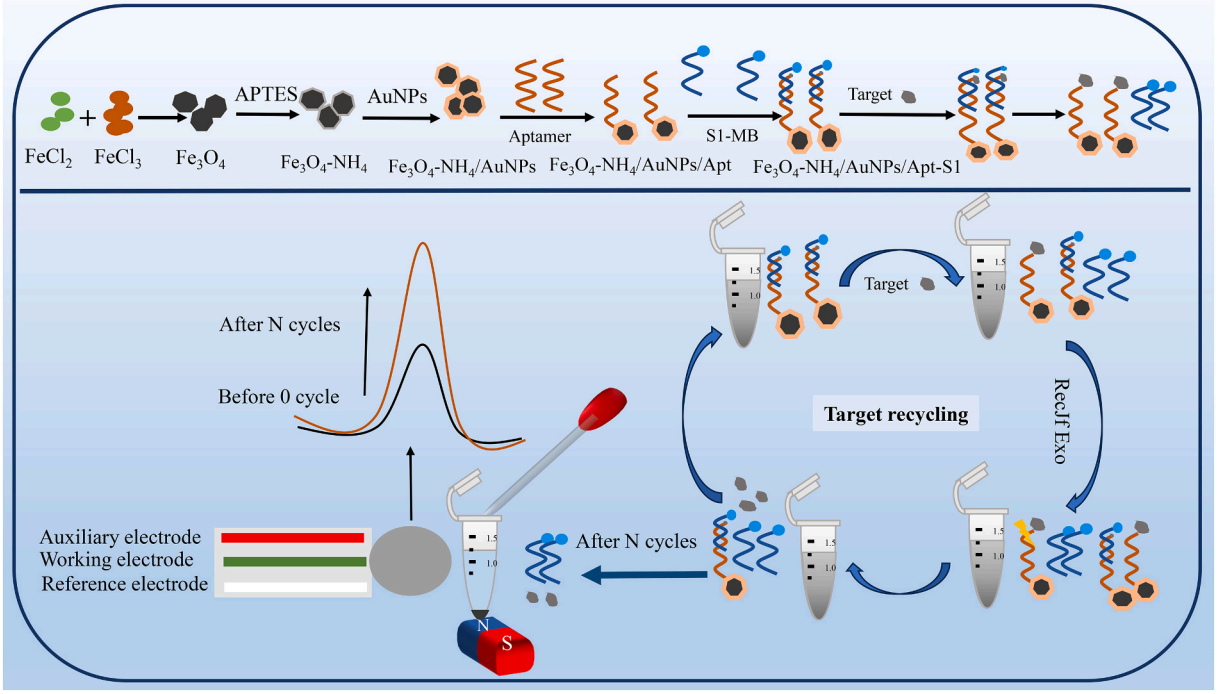

Fig. 1. Biosensor illustration of Fe_3O_4-NH_4/AuNPs/apt-S1 material synthesis and AFB1 detection.

following steps: Pipette 2.0 mL of the supernatant into a 5 mL centrifuge tube and evaporate to near dryness under nitrogen at room temperature. Then, 200 μL of hexane and 100 μL of trifluoroacetic acid were added to the tube, vortexed for 30 s, and derivatized for 15 min at 40 °C ± 1 °C in a constant temperature oven. After derivatization, the solution was evaporated to near dryness with nitrogen. It was then vortexed for 30 s to dissolve the residue with a 2.0 mL initial mobile phase and passed through a 0.22 μm membrane for sampling.

The chromatographic separation was carried out on an Agilent 1260 Infinity II system using a reversed-phase C_{18} column (4.6 × 250 mm, 5

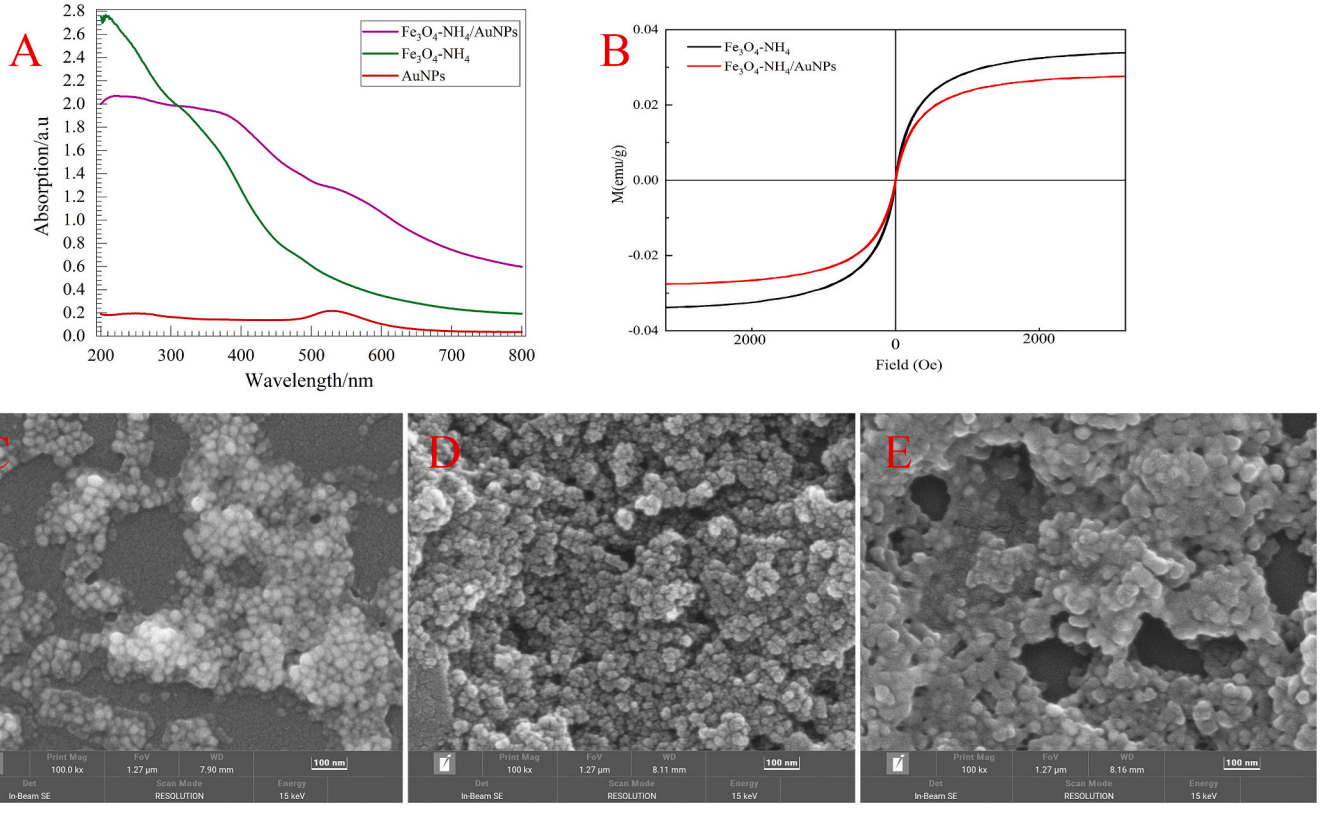

Fig. 2. UV − vis absorption of AuNPs, Fe_3O_4-NH_4 and Fe_3O_4-NH_4/ AuNPs (A); VSM of Fe_3O_4-NH_4, Fe_3O_4-NH_4/ AuNPs (B); SEM of AuNPs (C), Fe_3O_4-NH_4 (D), Fe_3O_4-NH_4/ AuNPs (E).

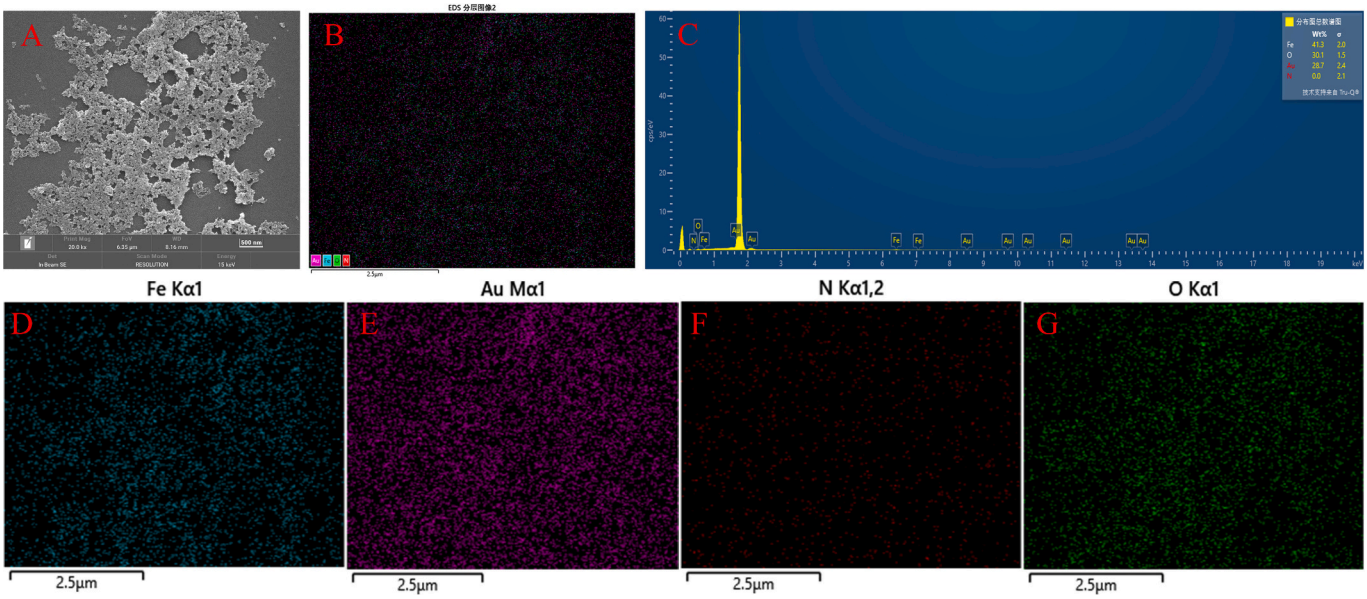

Fig. 3. EDS of Fe_3O_4-NH_4/ AuNPs (A-C); distributions of Fe, Au, N, and O elements in the EDS (D-G).

μm). The HPLC was equipped with a fluorescence detector, with an excitation wavelength of 360 nm and an emission wavelength of 440 nm. The mobile phase consisted of water (phase A) and acetonitrile-methanol (v: v, 1:1) (phase B). The elution gradient was: 0–3 min, 5–35%B, 3–6.2 min, 35–100%B, 6.2–7.5 min,100–50%B, 7.5–9 min, 50–24%B, 9–14 min, 24%B. The injection volume was 50 μL and the flow rate was 1.0 mL/min.

3. Results and discussion

3.1. Detection strategy of AFB1 biosensor

An electrochemical signal amplification system was developed based on the amplification strategy of AFB1 and Fe_3O_4-NH_4/AuNPs/apt-S1. Initially, Fe_3O_4 nanoparticles were synthesized using a co-precipitation method. These magnetic particles were subsequently functionalized with NH_4 groups via APTES, resulting in Fe_3O_4-NH_4. Next, AuNPs were linked to the amino groups on Fe_3O_4-NH_4, forming Fe_3O_4-NH_4/AuNPs. The aptamer was then attached to AuNPs through SH bonding, followed by the hybridization of S1, which had been modified with MB, to the complementary bases of the aptamer. In the presence of the target AFB1, AFB1 binds to the aptamer, forming a stable tetrameric structure and releasing S1. RecJf exonuclease specifically shears the aptamer, releasing AFB1, which then competes with the apt-S1 conjugate for the aptamer, initiating a new cycle. As this cycle repeats, the concentration of free S1 increases, resulting in an increased electrical signal, as illustrated in Fig. 1.

The KCl solution in the system provides K^+ and Cl^- ions, acting as mediators in the electrode reaction. The introduction of KCl enhances the electrolyte concentration, thereby increasing the rate and sensitivity of the electrochemical reaction. MB, a commonly used redox label and electron transfer medium with high stability, facilitates electron

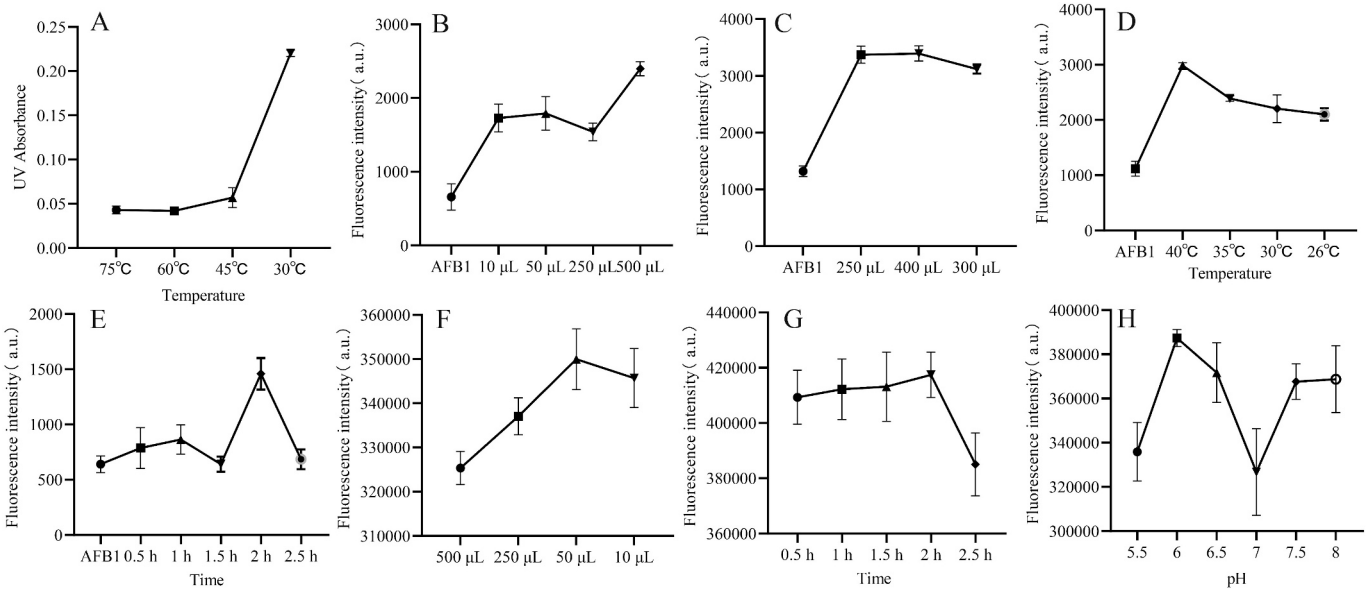

Fig. 4. Optimization the volume of AuNPs (A); Optimization the volume of apt, incubation temperature and time (B-E); Optimization the volume of S1, incubation time and pH (F-H).

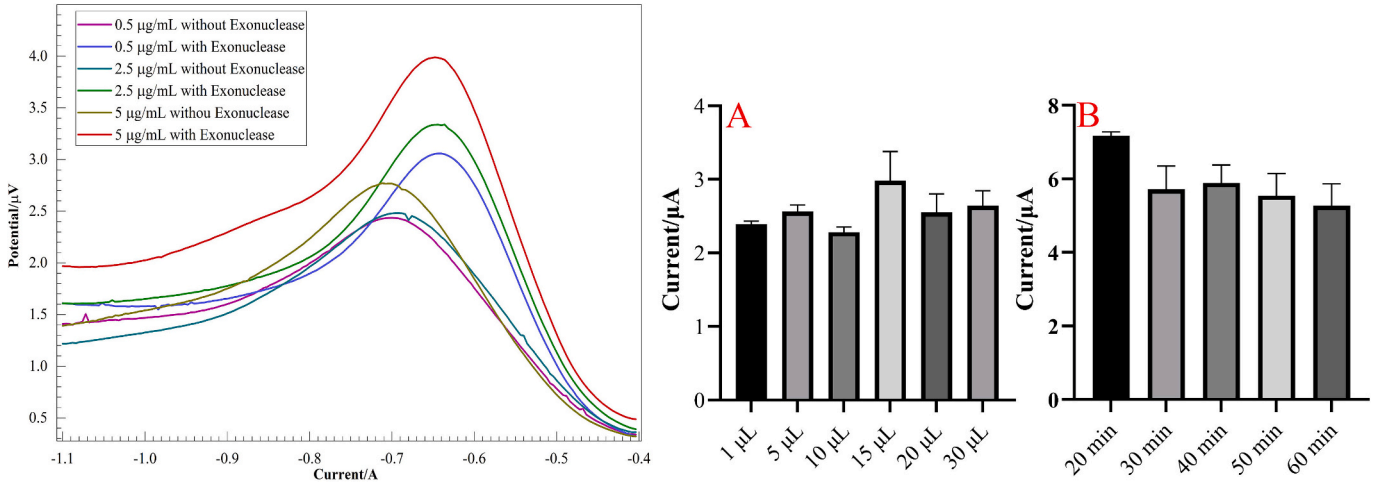

Fig. 5. Performance analysis of exonuclease, optimization the volume of exonuclease dosage (A), optimization of exonuclease incubation time (B).

generation and signal amplification in electrochemical biosensors (Bu et al., 2020; Li, Song, & Fan, 2010; Schoukroun-Barnes et al., 2016). On the electrode surface, MB undergoes a reduction reaction, converting to leucomethylene blue (LB) by absorbing two electrons (Chanarsa, Jakmunee, & Ounnunkad, 2022). As the concentration of S1 modified with MB increases, the efficiency of electron transfer increases, leading to an amplified current response.

3.2. Characterization of Fe_3O_4-NH_4/AuNPs

Ultraviolet spectrophotometry is a principal technique for determining the stability and development of metal nanoparticles (Karuppaiya et al., 2013). This method reveals distinct ultraviolet absorption peaks in a specific range. For gold nanoparticles with particle sizes between 2.5 and 100 nm, the surface plasmon resonance (SPR) absorption peaks are visible in the range of 520–580 nm (Haiss, Thanh, Aveyard, & Fernig, 2007). UV detection showed that the gold nanoparticles' peak appeared around 530 nm, while the peak of Fe_3O_4-NH_4 appeared around 360 nm. Following the modification of AuNPs, absorption peaks at both wavelengths were observed (Fig. 2A), suggesting the successful combination of AuNPs with Fe_3O_4-NH_4. The magnetic properties of Fe_3O_4-NH_4 and Fe_3O_4-NH_4/AuNPs nanoparticles were measured, revealing a difference in their saturation magnetic strengths of about 0.06 emu/g. This slight variation indicates that the magnetic properties of Fe_3O_4-NH_4 were not significantly degraded after AuNP modification, as shown in Fig. 2B. The superparamagnetism and magnetic induction properties showed that the amination effect did not significantly affect the superparamagnetism of the magnetic spheres (Guan et al., 2019).

Figs. 2C-E illustrate the morphology of AuNPs, Fe_3O_4-NH_4, and Fe_3O_4-NH_4/AuNPs under SEM. The images reveal sub-circular particles with a gradual increase in particle size. The particle sizes of AuNPs, Fe_3O_4-NH_4 and Fe_3O_4-NH_4/AuNPs in transmission electron microscopy were counted using image J software. The average particle sizes of AuNPs, Fe_3O_4-NH_4 and Fe_3O_4-NH_4/AuNPs were 21.36 nm, 47.91 nm and 116.19 nm, respectively (Supplementary Fig. 1). Fig. 3 shows that the energy dispersive spectrometer (EDS) detected Fe_3O_4-NH_4/AuNPs, demonstrating the distribution of Fe, O, N, and Au elements. The data indicates a higher detection of Au, suggesting successful attachment of gold nanoparticles to the surface of Fe_3O_4-NH_4 particles.

3.3. Optimization of analytical conditions

When 350 μL of AuNPs were sufficiently bound to a Fe_3O_4-NH_4 solution (1.5 mg/mL), the AuNPs in the solution supernatant appeared light pink. At the same incubation time, the least amount of free AuNPs in the supernatant was observed at an incubation temperature of 60 °C, with the lowest UV absorption (Fig. 4A). The incubation time was 12 h to ensure full binding of Fe_3O_4-NH_4 with AuNPs (Guan et al., 2019).

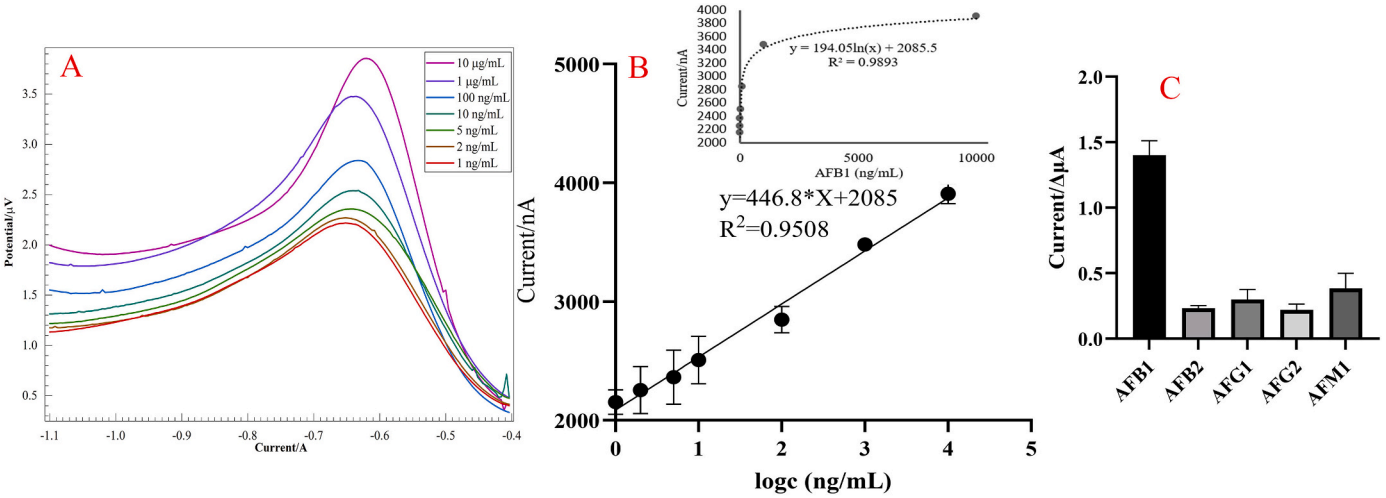

Fig. 6. Fe_3O_4-NH_4/AuNPs/apt-S1 detects the DPV response value of 1 ng-10 μg AFB1 in 0.1 M KCl solution and the corresponding standard curve and sensor selectivity for AFB1, AFB2, AFG1, AFG2 and AFM1.

Table 1
Comparison between this method and other reported techniques for the detection of AFB1.

Method	Journal	Linear range	Detection limit	Reference
FRET- Fluorescent biosensor)	Food Chemistry	10–400 nM	3.4 nM	(Sabet, Hosseini, Khabbaz, Dadmehr, & Ganjali, 2017)
Microarray technique and lateral flow immunoassay	Talanta	5–40 ppb (ng/mL)	1.3 (ng/mL)	(Charlermroj et al., 2021)
Lateral flow fluorescent strip immunosensor	Food Chemistry	1–19 ng/mL	1 ng/mL	(Jia et al., 2021)
Electrochemical method	Biosens Bioelectron	8 nM ~ 4 μM	2 nM	(Chao Wang, Li, & Zhao, 2019)
Aptamer-cross-linked hydrogel sensor	Food Chemistry: X	0–500 nM (0–847.79 μg/kg)	4.93 nM (8.395 μg/kg)	(Zheng et al., 2022)
Electrochemical method of amplification strategy		1–10,000 ng/mL	1.076 ng/mL (3.447 nM)	This work

Table 2
Comparison of the determination of AFB1 in peanut oil samples using both the Fe_3O_4-NH_4/AuNPs/apt-S1 sensor and HPLC ($n = 3$).

Spiked (ng/mL)	HPLC (ng/mL)	Recovery of HPLC (%)	The constructed sensor(ng/mL)	Recovery of sensor (%)	RSD (%)
1000	1003.0	100.3	1043.3	104.3	4.84
500	489.3	97.9	522.4	104.5	6.12
250	248.3	99.3	270.9	108.4	6.80
100	105.9	105.9	101.2	101.2	4.80

The aptamers were mixed and incubated with TCEP (1: 3; v, v) for 1 h at 37 °C to activate them. To optimize the volume of aptamers, incubation temperature, and incubation time, various volumes, temperatures, and times were tested. A fluorescence spectrophotometer with an excitation wavelength of 360 nm and emission wavelength of 450 nm was used to detect AFB1. When the aptamer binds sufficiently to AFB1, the amount of AFB1 in the supernatant rises to a plateau and then rises abruptly. The optimal volume of the aptamer is indicated at the plateau phase, which was 400 μL. When the aptamer binds to AFB1, the free AFB1 decreases, and the fluorescence intensity decreases. Therefore, the optimal incubation temperature was 26 °C and the optimal incubation time was 1.5 h (Fig. 4B-E).

Similarly, to optimize the volume of S1, the pH of incubation, and the incubation time, various volumes of S1, pH levels, and incubation times were tested. The fluorescence intensity of MB was detected using an enzyme marker at an excitation wavelength of 665 nm and an emission wavelength of 680 nm. When the binding of the complementary strand and the aptamer is complete and sufficient, the S1 in the supernatant increases, and the fluorescence intensity is high. Therefore, the optimal volume of S1 was 50 μL. When S1 and the aptamer are well-bound, free S1 decreases, and fluorescence intensity decreases. Thus, the optimal incubation time was 2.5 h, and the optimal incubation pH was 7.0 (Fig. 4F-H).

3.4. Feasibility of exonucleases in electrochemical sensors

To confirm the effect of exonucleases in electrochemical sensors, we explored the electrochemical behavior with and without exonucleases. Using the optimized synthesis conditions of Fe_3O_4-NH_4/AuNPs/apt-S1, we set up three different AFB1 concentrations both with and without exonuclease. The results are shown in Fig. 5. The use of exonuclease was performed according to the instructions.

After confirming the effect of exonuclease on the electrochemical sensor, the optimal reaction temperature of this enzyme is 37 °C according to the instructions. The Fe_3O_4-NH_4/AuNPs/apt-S1-AFB1 reaction system was incubated with different volumes (1, 5, 10, 15, 20, 30 μL) and incubation times (20, 30, 40, 50, 60 min) to optimize the volume of RecJf exonuclease and the incubation time. The reaction was terminated by incubating at 65 °C for 20 min. The results indicated that the optimal volume of RecJf exonuclease was 15 μL, with an incubation time of 20 min (Fig. 5A and B).

3.5. Evaluation of sensor performance

The sensor can detect different concentrations of AFB1 under optimized conditions. Higher concentrations of AFB1 result in more free S1 modified with MB after the enzymatic cycling reaction, leading to a stronger electrical signal in DPV. As shown in Fig. 6, there is a linear relationship between AFB1 concentrations from 1 ng to 10 μg, described by the regression eq. $I(nA) = 446.8 \times \log c + 2085$ (where I is the peak current and c is the concentration of AFB1, respectively). The correlation coefficient was 0.9508, and the detection limit was 3.447 nM.

The International Union of Pure and Applied Chemistry (IUPAC) recommends a signal-to-noise ratio of 3 and calculating the limit of detection (LOD). It uses the standard deviation (Sb) of the blank signal and the slope (S) of the calibration curve ($LOD = 3Sb/S = 3 \times 0.1603/0.4468 = 1.076$ ng/mL $= 3.447$ nM). Table 1 compares the performance of the sensors with other studies to more accurately and comprehensively reflect the performance of current AFB1 sensors.

3.6. Selectivity and stability of electrochemical sensors

The selectivity and stability of the biosensor were evaluated using the DPV method. A solution of 1 μg/mL AFB1 was used as the standard for detection. Current values were measured at 0, 4, 8, 12, and 24 h, with an RSD value of 1.81%. The current value was repeated 8 times by taking 1 μg/mL at 0 h from the standard curve and its RSD value was 1.64%. The selectivity of the electrochemical sensor was examined using AFB2 (2.15 μg/mL), AFM1 (2.5 μg/mL), AFG1 (2.0 μg/mL), and AFG2 (2.0 μg/mL) as interferents. Fig. 6C shows the high intensity of the AFB1 signal compared to other mycotoxins. These results confirm the sensor's good stability, repeatability, and selectivity.

3.7. Real sample detection

This electrochemical sensor was used to detect AFB1 in peanut oil to compare its accuracy in detecting real samples. Peanut oil was extracted from AFB1 while adding a certain amount of AFB1 standard, then derivatized AFB1 and detected using a HPLC fluorescence detector, resulting in an RSD<6.8% and satisfactory recoveries (Table 2).

4. Conclusion

A Fe_3O_4-NH_4/AuNPs/apt-S1 electrochemical sensor was successfully developed for detecting AFB1 in peanut oil. This sensor features high sensitivity, straightforward operation, and economical processing costs. The aptamer in this sensor is specific for AFB1, and the inclusion of RecJf exonuclease enables electrical signal amplification. Additionally, the utilization of screen-printed electrodes further simplifies and facilitates the detection process. The Fe_3O_4 with magnetic properties allows for rapid separation of solids and liquids without large-scale instruments. The sensor has a large linear range (1 ng-10 μg) and a low detection limit (3.447 nM). The stability and repeatability of the sensor in this work are remarkable, with RSD<2%. The sensor's application to AFB1 detection in peanut oil has been validated and compared favorably to HPLC, with RSD<6.8% and satisfactory recoveries. In summary, this method offers

an innovative approach to monitoring AFB1 levels in food and other industries to ensure food safety.

Supplementary data to this article can be found online at https://doi.org/10.1016/j.fochx.2024.101605.

CRediT authorship contribution statement

Hua Zheng: Writing – original draft, Writing – review & editing, Data curation. **Linlin Feng:** Data curation. **Zheng Huang:** Conceptualization, Writing – review & editing, Writing – original draft, Data curation. **Ziwei Zou:** Data curation. **Xiaolong Ma:** Data curation. **Zipping Pan:** Methodology. **Jinfeng Li:** Methodology. **Jinxia Wu:** Methodology. **Mei Li:** Investigation. **Zhiheng Su:** Resources, Project administration, Funding acquisition.

Declaration of competing interest

The authors declare that they have no known competing financial interests or personal relationships that could have appeared to influence the work reported in this paper.

Data availability

The data that has been used is confidential.

Acknowledgement

This research was financially supported by the Guangxi First Class Discipline (Pharmacy) Construction Project (GXFCDG-PS-2018).

References

Abdolmaleki, K., Javanmardi, F., Gavahian, M., Phimolsiripol, Y., Ruksiriwanich, W., Mir, S. A., & Mousavi Khaneghah, A. (2022). Emerging technologies in combination with probiotics for aflatoxins removal: An updated review. *International Journal of Food Science & Technology, 57*(9), 5712–5721. https://doi.org/10.1111/ijfs.15926

Abedi, R., Raoof, J. B., Mohseni, M., & Bagheri Hashkavayi, A. (2023). A signal-off aptasensor for the determination of *Acinetobacter baumannii* by using methylene blue as an electrochemical probe. *Microchimica Acta, 190*(8). https://doi.org/10.1007/s00604-023-05901-0

Bu, S., Wang, K., Li, Z., Wang, C., Hao, Z., Liu, W., & Wan, J. (2020). An electrochemical biosensor based on methylene blue-loaded nanocomposites as signal-amplifying tags to detect pathogenic bacteria. *The Analyst, 145*(12), 4328–4334. https://doi.org/10.1039/d0an00470g

Chanarsa, S., Jakmunee, J., & Ounnunkad, K. (2022). A sandwich-like configuration with a signal amplification strategy using a methylene blue/aptamer complex on a heterojunction 2D MoSe2/2D WSe2 electrode: Toward a portable and sensitive electrochemical alpha-fetoprotein immunoassay. *Frontiers in Cellular and Infection Microbiology, 12*. https://doi.org/10.3389/fcimb.2022.916357

Charlermroj, R., Phuengwas, S., Makornwattana, M., Sooksimuang, T., Sahasithiwat, S., Panchan, W., & Karoonuthaisiri, N. (2021). Development of a microarray lateral flow strip test using a luminescent organic compound for multiplex detection of five mycotoxins. *Talanta, 233*. https://doi.org/10.1016/j.talanta.2021.122540

Chavarría, G., Molina, A., Leiva, A., Méndez, G., Wong-González, E., Cortés-Muñoz, M., & Granados-Chinchilla, F. (2017). Distribution, stability, and protein interactions of aflatoxin M 1 in fresh cheese. *Food Control, 73*, 581–586. https://doi.org/10.1016/j.foodcont.2016.09.005

Dean, L. (2021). Peanut protein-processes and applications. A review. *Journal of Nutrition & Food Sciences, 2021*(44), 031.

Fakhri, Y., Omar, S. S., Mehri, F., Hoseinvandtabar, S., & Mahmudiono, T. (2023). Global systematic review and meta-analysis on prevalence and concentration of aflatoxins in peanuts oil and probabilistic risk assessment. *Reviews on Environmental Health, 38*(4), 697–712. https://doi.org/10.1515/reveh-2022-0075

Fang, G., Chen, H., Zhang, Y., & Chen, A. (2016). Immobilization of pectinase onto Fe3O4@SiO2–NH2 and its activity and stability. *International Journal of Biological Macromolecules, 88*, 189–195. https://doi.org/10.1016/j.ijbiomac.2016.03.059

Fasihi-Ramandi, M., Bayat, G., Kachuei, R., & Golmohammadi, R. (2023). (2023). Effects of aflatoxin B1 exposure on sperm in rodents: A systematic review and meta-analysis. *International Journal of Environmental Health Research, 33*(12), 1629–1639. https://doi.org/10.1080/09603123.2022.2113766

Frns. (1973). Controlled nucleation for the regulation of the particle size in monodisperse gold suspensions. *Nature Physical Science, 241*(105), 20–22.

Guan, H., Han, B., Gong, D., Song, Y., Liu, B., & Zhang, N. (2019). Colorimetric sensing for ascorbic acid based on peroxidase-like of GoldMag nanocomposites. *Spectrochimica Acta Part A: Molecular and Biomolecular Spectroscopy, 222*. https://doi.org/10.1016/j.saa.2019.117277

Haiss, W., Thanh, N. T., Aveyard, J., & Fernig, D. G. (2007). (2007). Determination of size and concentration of gold nanoparticles from UV-vis spectra. *Analytical Chemistry, 79*(11), 4215–4221. https://doi.org/10.1021/ac0702084

Han, S., Liu, W., Yang, S., & Wang, R. (2019). Facile and label-free electrochemical biosensors for MicroRNA detection based on DNA origami nanostructures. *ACS Omega, 4*(6), 11025–11031. https://doi.org/10.1021/acsomega.9b01166

Jia, B., Liao, X., Sun, C., Fang, L., Zhou, L., & Kong, W. (2021). Development of a quantum dot nanobead-based fluorescent strip immunosensor for on-site detection of aflatoxin B1 in lotus seeds. *Food Chemistry, 356*. https://doi.org/10.1016/j.foodchem.2021.129614

Karuppaiya, P., Satheeshkumar, E., Chao, W.-T., Kao, L.-Y., Chen, E. C.-F., & Tsay, H.-S. (2013). Anti-metastatic activity of biologically synthesized gold nanoparticles on human fibrosarcoma cell line HT-1080. *Colloids and Surfaces B: Biointerfaces, 110*, 163–170. https://doi.org/10.1016/j.colsurfb.2013.04.037

Khadieva, A., Mostovaya, O., Padnya, P., Kalinin, V., Grishaev, D., Tumakov, D., & Stoikov, I. (2021). Arylamine analogs of methylene blue: Substituent effect on aggregation behavior and DNA binding. *International Journal of Molecular Sciences, 22*(11). https://doi.org/10.3390/ijms22115847

Lei, M., Zhang, N., & Qi, D. (2013). In vitro investigation of individual and combined cytotoxic effects of aflatoxin B1 and other selected mycotoxins on the cell line porcine kidney 15. *Experimental and Toxicologic Pathology, 65*(7–8), 1149–1157. https://doi.org/10.1016/j.etp.2013.05.007

Li, D., Song, S., & Fan, C. (2010). (2010). Target-responsive structural switching for nucleic acid-based sensors. *Accounts of Chemical Research, 43*(5), 631–641. https://doi.org/10.1021/ar900245u

Marchese, S., Polo, A., Ariano, A., Velotto, S., Costantini, S., & Severino, L. (2018). Aflatoxin B1 and M1: biological properties and their involvement in cancer development. *Toxins, 10*(6). https://doi.org/10.3390/toxins10060214

Miao, X., Li, Z., Zhu, A., Feng, Z., Tian, J., & Peng, X. (2016). Ultrasensitive electrochemical detection of protein tyrosine kinase-7 by gold nanoparticles and methylene blue assisted signal amplification. *Biosensors and Bioelectronics, 83*, 39–44. https://doi.org/10.1016/j.bios.2016.04.032

Qian, J., Ren, C., Wang, C., Chen, W., Lu, X., Li, H., & Wang, K. (2018). Magnetically controlled fluorescence aptasensor for simultaneous determination of ochratoxin a and aflatoxin B1. *Analytica Chimica Acta, 1019*, 119–127. https://doi.org/10.1016/j.aca.2018.02.063

Rushing, B. R., & Selim, M. I. (2019). Aflatoxin B1: A review on metabolism, toxicity, occurrence in food, occupational exposure, and detoxification methods. *Food and Chemical Toxicology, 124*, 81–100. https://doi.org/10.1016/j.fct.2018.11.047

Sabet, F. S., Hosseini, M., Khabbaz, H., Dadmehr, M., & Ganjali, M. R. (2017). FRET-based aptamer biosensor for selective and sensitive detection of aflatoxin B1 in peanut and rice. *Food Chemistry, 220*, 527–532. https://doi.org/10.1016/j.foodchem.2016.10.004

Schoukroun-Barnes, L. R., Macazo, F. C., Gutierrez, B., Lottermoser, J., Liu, J., & White, R. J. (2016). Reagentless, structure-switching, electrochemical aptamer-based sensors. *Annual Review of Analytical Chemistry, 9*(1), 163–181. https://doi.org/10.1146/annurev-anchem-071015-041446

Tan, H., Ma, L., Guo, T., Zhou, H., Chen, L., Zhang, Y., & Yu, Y. (2019). A novel fluorescence aptasensor based on mesoporous silica nanoparticles for selective and sensitive detection of aflatoxin B1. *Analytica Chimica Acta, 1068*, 87–95. https://doi.org/10.1016/j.aca.2019.04.014

Tani, A., Thomson, A. J., & Butt, J. N. (2001). Methylene blue as an electrochemical discriminator of single- and double-stranded oligonucleotides immobilised on gold substrates. *The Analyst, 126*(10), 1756–1759. https://doi.org/10.1039/b104260m

Tosun, H., & Ayyıldız, T. (2013). Occurrence of aflatoxin M1 in organic dairy products. *Quality Assurance & Safety of Crops and Food, 5*(3), 215–219. https://doi.org/10.3920/qas2012.0147

Vardevanyan, P. O., Antonyan, A. P., Parsadanyan, M. A., Shahinyan, M. A., & Petrosyan, N. H. (2021). Study of interaction of methylene blue with DNA and albumin. *Journal of Biomolecular Structure and Dynamics, 40*(17), 7779–7785. https://doi.org/10.1080/07391102.2021.1902397

Wang, C., Li, Y., & Zhao, Q. (2019). A signal-on electrochemical aptasensor for rapid detection of aflatoxin B1 based on competition with complementary DNA. *Biosensors and Bioelectronics, 144*. https://doi.org/10.1016/j.bios.2019.111641

Wang, C., Qian, J., An, K., Ren, C., Lu, X., Hao, N., & Wang, K. (2018). Fabrication of magnetically assembled aptasensing device for label-free determination of aflatoxin B1 based on EIS. *Biosensors and Bioelectronics, 108*, 69–75. https://doi.org/10.1016/j.bios.2018.02.043

Wang, P., Ding, L., Zhang, Y., & Jiang, X. (2023). A novel aptamer biosensor based on a localized surface plasmon resonance sensing chip for high-sensitivity and rapid enrofloxacin detection. *Biosensors, 13*(12). https://doi.org/10.3390/bios13121027

Wang, Y., Xu, J., Ma, C., Li, S., Yu, J., Ge, S., & Yan, M. (2014). A chemiluminescence excited photoelectrochemistry aptamer-device equipped with a tin dioxide quantum dot/reduced graphene oxide nanocomposite modified porous au-paper electrode. *Journal of Materials Chemistry B, 2*(22), 3462–3468. https://doi.org/10.1039/c4tb00233d

Wild, C. P., & Gong, Y. Y. (2010). Mycotoxins and human disease: A largely ignored global health issue. *Carcinogenesis, 31*(1), 71–82. https://doi.org/10.1093/carcin/bgp264

Wu, Y., Baker, S. L., & Lai, R. Y. (2017). Effects of DNA probe length on the performance of a dynamics-based electrochemical hg(II) sensor. *Electroanalysis, 29*(10), 2239–2245. https://doi.org/10.1002/elan.201700314

Wu, Y., & Lai, R. Y. (2017). Tunable signal-off and signal-on electrochemical cisplatin sensor. *Analytical Chemistry, 89*(18), 9984–9989. https://doi.org/10.1021/acs.analchem.7b02353

Xu, Y., Wang, X., Ding, C., & Luo, X. (2021). Ratiometric antifouling electrochemical biosensors based on multifunctional peptides and MXene loaded with au nanoparticles and methylene blue. *ACS Applied Materials & Interfaces, 13*(17), 20388–20396. https://doi.org/10.1021/acsami.1c04933

Yu, Z.-G., Sutlief, A. L., & Lai, R. Y. (2018). Towards the development of a sensitive and selective electrochemical aptamer-based ampicillin sensor. *Sensors and Actuators B: Chemical, 258*, 722–729. https://doi.org/10.1016/j.snb.2017.11.193

Zhang, L. Z., & Tang, G.-Q. (2004). The binding properties of photosensitizer methylene blue to herring sperm DNA: A spectroscopic study. *Journal of Photochemistry and Photobiology B: Biology, 74*(2–3), 119–125. https://doi.org/10.1016/j.jphotobiol.2004.03.005

Zheng, M., Liu, H., Ye, J., Ni, B., Xie, Y., & Wang, S. (2022). Target-responsive aptamer-cross-linked hydrogel sensors for the visual quantitative detection of aflatoxin B1 using exonuclease I-triggered target cyclic amplification. *Food Chemistry: X, 15*. https://doi.org/10.1016/j.fochx.2022.100395